DOI: 10.1002/ejic.200801185

Tuning the Emission Color of Iridium(III) Complexes with Ancillary Ligands: A Combined Experimental and Theoretical Study

Xin Gu,[a] Teng Fei,[a] Houyu Zhang,*[a] Hai Xu,[a] Bing Yang,[a] Yuguang Ma,*[a] and Xiaodong Liu[b]

Keywords: Iridium / Ligand effects / Dyes/Pigments / Density functional calculations / Charge transfer

A series of iridium(III) complexes [Ir(dfppy)$_2$(L^X)] {dfppy = 2-(2,4-difluorophenyl)pyridine, L^X = acac, FIr(acac); dbm, FIr(dbm); natfac, FIr(natfac); acac = acetylacetonate, dbm = dibenzoylmethanane, natfac = 1-naphthoyl-3,3,3-trifluoroacetone} have been synthesized and characterized by elemental analysis, NMR and IR spectroscopy, and mass spectrometry. The cyclic voltammetric, absorption, and emission properties of these complexes have been systematically investigated. Density functional theory (DFT) and time-dependent DFT (TD-DFT) calculations have been performed to investigate the ground- and excited-state properties of these complexes to provide an insight into their structural, electronic, and optical properties. The results of this work provide further evidence regarding how and to what extent the substituents on the ancillary ligand L^X influence the emission properties of [Ir(dfppy)$_2$(L^X)] complexes.

Introduction

Considerable research efforts have been focused on phosphorescent transition metal complexes for use as room-temperature dyes in the past few years.[1] These materials have intriguing photophysical, photochemical, and excited-state redox properties and high internal quantum efficiencies (η_{int}) which, in principle, can reach almost 100%.[2] They also possess strong spin-orbit couplings, which allow fast intersystem crossing among the low-lying electronic states.[3] The motivations for using those emissive complexes include fundamental research on excited-state charge- and energy-transfer as well as potential applications in sensors[4] and as organic light-emitting diodes (OLEDs).[5]

Phosphorescent d^6 metal complexes of Ir^{III},[6] Ru^{II},[7] and Os^{II}[8] have shown high efficiency in OLEDs. Among these complexes, iridium(III) complexes are regarded as the most effective materials in OLEDs as they exhibit a high thermal stability, a short lifetime in the excited state,[9] and are tunable in the blue to red region upon modification of the ligand[10] or by introducing a variety of electron donors or acceptors into the ligand.[11] To achieve wide-range color emission for use in full color displays, many different classes of homoleptic [Ir(C^N)$_3$] and heteroleptic [Ir(C^N)$_2$L^X] iridium(III) complexes have been developed (C^N is a cyclometalating ligand and L^X is an ancillary ligand), although previous studies have tended to place more emphasis on modifying the cyclometalating ligand C^N to obtain different colors.[5b,12] It used to be believed that ancillary ligands play a minor and supporting role in the coordination sphere. However, Park[13] and Chou[14] have shown that the ancillary ligands are also able to adjust the emission color of complexes. Likewise, spectroscopic studies have revealed that ancillary ligands alter the ^{1}MLCT energy by changing the HOMO energy level,[15] and theoretical calculations have indicated that strong-field ancillary L^X ligands lengthen the bonds between the C^N ligands and the metal, thus altering the electronic properties of the metal complexes.[16] Research on ancillary ligands has therefore attracted more and more attention.

Many questions regarding how and to what extent ancillary ligands affect the optical properties of metal complexes remain unsolved, although several recent reports have investigated the effects of ancillary ligands from both an experimental and a theoretical perspective. The function of the ancillary ligands in these complexes remains elusive, and their role in tuning the emission color is still under debate. It is therefore vital to investigate their role further to gain an insight into the interaction between the ancillary ligands and the metal and hence understand the relationship between the structures and properties. The optical properties of cyclometalated Ir^{III} complexes are strongly dependent on the characteristics of their ground and low-lying excited states. Density functional theory (DFT) provides a means to evaluate a variety of ground-state properties with an accuracy close to post-HF methods.[17] Similarly, time-dependent DFT (TD-DFT) calculations make it possible

[a] State Key Laboratory of Supramolecular Structure and Materials, Jilin University,
Changchun 130012, P. R. China
Fax: +86-431-85168480
E-mail: houyuzhang@jlu.edu.cn
ygma@jlu.edu.cn
[b] College of chemistry, Jilin University,
Changchun 130012, P. R. China

to calculate the vertical electronic excitation for the excited states.[18]

Herein we demonstrate color tuning by ancillary ligands in a joint experimental and theoretical study and report the synthesis and characterization of a series of iridium(III) complexes [Ir(dfppy)$_2$(L^X)] with acac, dbm, and natfac (acac = acetylacetonate, dbm = dibenzoylmethanane, natfac = 1-naphthoyl-3,3,3-trifluoroacetone) as ancillary ligands (see Figure 1). The redox behavior and optical properties of these complexes are systemically investigated, and DFT calculations are performed to gain a better understanding of the role of ancillary ligands in color tuning. Although the structures we investigated are not particularly novel from a structural point of view, our attention was focused on the interaction of the ancillary ligands with the metal from a combined experimental and DFT viewpoint. Tuning the emission color of these complexes can easily be achieved by systematically varying the substituents on L^X.

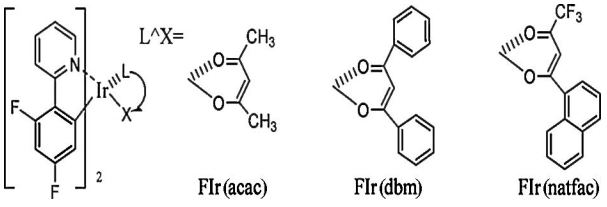

Figure 1. Structures of Ir complexes FIr(acac), FIr(dbm), and FIr(natfac).

Results and Discussion

Preparation and Photophysical Properties

All synthetic procedures were carried out under an inert gas atmosphere. The cyclometalated chloride-bridged dimer [(dfppy)$_2$Ir(μ-Cl)$_2$Ir(dfppy)$_2$] was synthesized according to a procedure described in the literature[19] by refluxing $IrCl_3 \cdot nH_2O$ with the cyclometalating ligand in a mixture of 2-ethoxyethanol and water. The chloride-bridged dimer complexes were refluxed under N_2 in 2-ethoxythanol, and the precipitate formed after cooling to room temperature was filtered off and washed with water and diethyl ether. The crude product was subjected to column chromatography on silica gel, eluting with dichloromethane, to provide the desired product in quantitative yield (see Exp. Sect.). The chemical structures of FIr(acac) (**1**), FIr(dbm) (**2**), and FIr(natfac) (**3**) are shown in Figure 1. Figure 2 shows the absorption spectra of FIr(acac), FIr(dbm), and FIr(natfac) in dichloromethane solution. Absorptions below 370 nm are ascribed to metal-perturbed ligand-centered absorptions on the basis of relatively higher extinction coefficients of the bands. The absorptions at long wavelength (370–480 nm) are weak (molar absorption coefficients of less than 1×10^{-4} M^{-1}cm^{-1}) and broad and are assigned to metal-to-ligand charge transfer (MLCT) absorptions. The emission spectra for the complexes in PMMA films are shown in Figure 3. The photoluminescence spectra of the complexes exhibit a large bathochromic shift from blue [482 nm for FIr(acac)] to orange-red [586 nm for FIr(natfac)] as the ancillary ligand changes. FIr(acac) exhibits strong emission at room temperature in solution, whereas emission is very weak for FIr(dbm) and FIr(natfac).

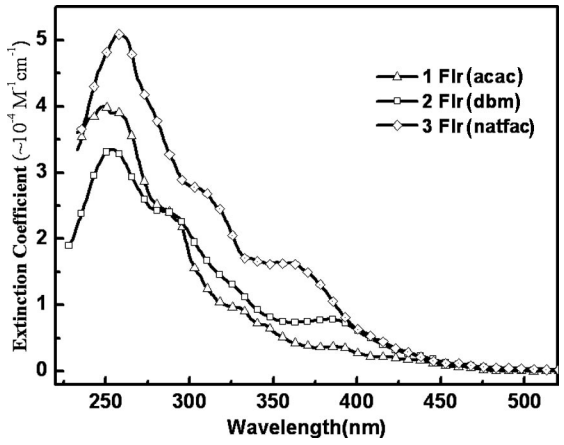

Figure 2. Absorption spectra of complexes **1**–**3** in CH_2Cl_2 solution.

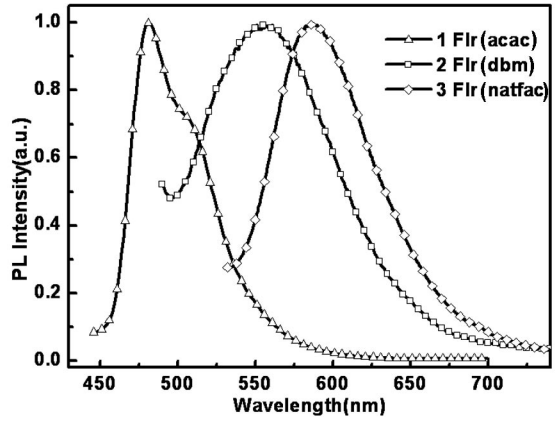

Figure 3. Emission spectra of complexes **1**–**3** in PMMA films.

Electrochemistry

The electrochemical properties of the Ir^{III} complexes were examined by cyclic voltammetry (CV) in a standard one-compartment, three-electrode electrochemical cell (BAS 100B/W, Bioanalytical Systems). A summary of the redox potentials of the complexes is given in Table 1. It is generally accepted that the oxidation of Ir^{III} species involves the iridium moiety of the complexes and that the HOMOs are mostly due to the d orbitals of iridium with some π-orbital contributions from the ligand. The LUMO in this kind of complex is due either to dfppy or the ancillary ligands. This electrochemical behavior is consistent with a description of the ligand-localized LUMO states and a HOMO with substantial metal character, as can be seen in our theoretical calculations below. The HOMO–LUMO energy gaps are 3.22, 2.34, and 2.04 eV for complexes **1**–**3**,

respectively, which is consistent with the results from the maximum emission wavelength. The effect of the ancillary ligands on changing the energy gaps of the complexes is therefore verified by the electrochemical measurements.

Table 1. Electrochemical and photophysical properties of Ir complexes **1**–**3**.

	E^{Ox}_{onset} [V]	HOMO [eV]	E^{Red}_{onset} [V]	LUMO [eV]	Energy gap [eV]	$\lambda_{max,Em}$ [nm]	T_1[a] [eV]
1	0.82	–5.42	–2.40	–2.20	3.22	482	2.57
2	0.32	–4.92	–2.02	–2.58	2.34	557	2.23
3	0.41	–5.01	–1.63	–2.97	2.04	586	2.11

[a] The triplet energy was estimated from λ_{max} of the phosphorescence spectra.

Geometries and Orbital Configurations

To provide a quantum chemical insight into these complexes, the DFT method was employed to investigate their ground-state electronic structures and orbital configurations. The optimized ground-state structures of FIr(acac), FIr(dbm), and FIr(natfac) are shown in Figure 4 and selected geometrical parameters are listed in Table 2, together with available experimental X-ray diffraction data for FIr(dbm). The common feature in all complexes is that the ancillary ligands bind to the metal center through two Ir–O bonds despite having different substituents on atoms C3 and C5. The calculated bond lengths are in good agreement with available crystal structural data (standard deviation of about 0.0038 Å)[20] and are comparable with previously calculated results.[16,21]

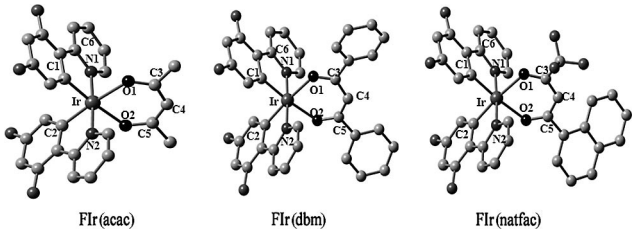

Figure 4. Optimized geometries of FIr(acac), FIr(dbm), and FIr(natfac) with two N atoms from dfppy in the *trans* positions (saturated H atoms are not shown).

The calculated metal–ligand Ir–C (about 2.002 Å) and Ir–N (about 2.064 Å) bond lengths in all three complexes are almost the same, whereas the Ir–O bond lengths vary slightly as the ancillary ligands change. The phenyl group in dbm exhibits a stronger conjugating effect on the C=O bond than the methyl group in acac, thus leading to higher electron density on the oxygen atom and a shorter Ir–O bond. The substituent effect of a phenyl group on the ligand has been observed previously.[22] In the case of FIr(natfac), however, the electron-withdrawing CF_3 group in natfac removes electron density from the metal and the naphthyl group delocalizes the electron density effectively, which weakens the interaction between the central Ir atom and the natfac ligand and means that the Ir–O bond is lengthened. The effect of the strong π-electron delocalization of the naphthyl group can clearly be seen in the contour plots for the HOMO-1 of FIr(natfac) in Figure 6. The asymmetric substitution by trifluoromethyl and naphthyl groups in this complex makes Ir–O_1 (2.194 Å) and Ir–O_2 (2.205 Å) distinguishable. The calculated bond angles and dihedral angles also show only a slight change of about 1°. It is therefore clear that the ancillary ligands do not significantly alter the geometries, which is a reflection of the similarities between the ancillary ligands.

Table 2. Main parameters of complexes **1**–**3** in the ground state (S_0) optimized at the B3LYP level, together with experimental values for FIr(dbm).

	FIr(acac)	FIr(dbm)	FIr(natfac)	FIr(dbm)[exp]
Bond lengths [Å]				
Ir–C1	2.002 (1.998),[a] (2.002)[b]	2.002	2.001	1.974
Ir–N1	2.062 (2.031),[a] (2.062)[b]	2.065	2.066	2.033
Ir–C2	2.002 (1.998)[a]	2.003	2.001	2.005
Ir–N2	2.062 (2.031)[a]	2.061	2.067	2.027
Ir–O1	2.194 (2.147),[a] (2.190)[b]	2.186	2.194	2.149
Ir–O2	2.194 (2.147)[a]	2.186	2.205	2.121
Bond angles [°]				
O1–Ir–O2	86.4	86.1	86.0	89.1
C1–Ir–C2	93.5	92.6	92.7	90.4
C3–C4–C5	127.3	127.5	125.9	128.1
Dihedral angles [°]				
C6–N1–Ir–O1	–85.9	–87.2	–87.1	–90.8

[a] Values in parentheses are from ref.[16]. [b] Values in parentheses are from ref.[21].

The frontier molecular orbitals of the ground state (S_0) are very important because they are closely related to the electronic transitions pertaining to the absorption and emission processes. By analyzing the frontier molecular orbitals, we can therefore gain a better insight into the electronic structures of the complexes. The HOMO and LUMO energy levels of dfppy, acac, dbm, and natfac are shown in Figure 5. As we can see, the HOMO levels of the three ancillary ligands and the cyclometalating ligand dfppy are similar in energy, whereas the LUMO energies of the ancillary ligands are significantly influenced by the substitution effect. Thus, the LUMO energies of dbm and natfac are dramatically lowered to –2.00 and –2.48 eV, respectively, which means that the energy gaps of the ancillary ligands range from 5.35 to 3.78 eV. The electronic effects produced upon incorporation of electron-donating and electron-withdrawing groups into the ligand structures therefore have a remarkable influence on the orbital energies, which in turn results in different photophysical behaviors of their metal complexes.

The frontier molecular orbital energies for the three complexes, along with their composition and main bonding types, are listed in Table 3, and the contour plots of the two highest HOMOs and two lowest LUMOs of the Ir complexes are shown in Figure 6. The HOMOs of the complexes are mainly formed from the metallic "t_{2g}" d orbitals

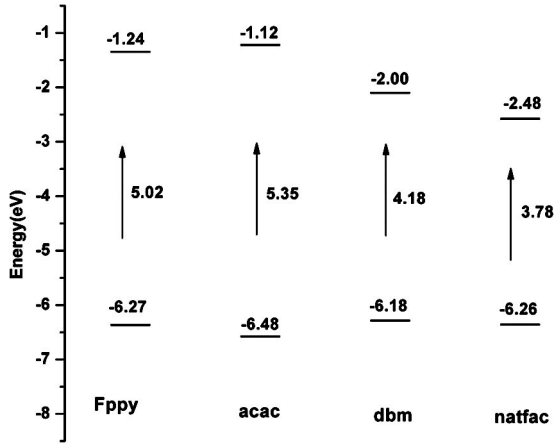

Figure 5. Comparison of the HOMO and LUMO energy levels and the energy gaps in ligands dfppy, acac, dbm, and natfac.

and the π orbitals of the ligand dfppy, with d components of 52.2%, 51.4%, and 50.8% for FIr(acac), FIr(dbm), and FIrntfac, respectively. Because of the lower HOMO level of ligand dfppy, the HOMO energies of the complexes are determined by the percentage dfppy orbital composition.

Table 3. Molecular orbital energy and composition in the ground state for complexes **1**–**3** at the B3LYP level.

	Orbital[a]	Energy [eV]	MO composition (%) Ir	C^N	LX	Main bonding type
1	L+2	–0.93	2.03	97.1	0.885	π*(dfppy)
	L+1	–1.48	5.28	93.1	1.63	π*(dfppy)
	L	–1.48	4.88	93.2	1.87	π*(dfppy)
	H	–5.25	52.2	41.6	6.22	d(Ir) + π(*dfppy*)
	H-1	–5.58	38.9	11.1	50.0	d(Ir) + π(*acac*)
	H-2	–6.04	0.769	93.5	5.71	π(dfppy)
	H-3	–6.05	36.1	59.7	4.13	d(Ir) + π(*dfppy*)
2	L+2	–1.46	5.33	89.9	4.73	π*(dfppy)
	L+1	–1.49	5.25	93.0	1.78	π*(dfppy)
	L	–1.69	2.22	8.31	89.5	π*(*dbm*)
	H	–5.27	51.4	40.6	8.00	d(Ir) + π(*dfppy*)
	H-1	–5.56	33.8	10.1	56.2	π(*dbm*) + d(Ir)
	H-2	–6.03	27.1	63.6	9.31	π(*dfppy*) + d(Ir)
	H-3	–6.05	24.5	68.1	7.40	π(*dfppy*) + d(Ir)
3	L+2	–1.60	5.24	91.1	3.64	π*(dfppy)
	L+1	–1.63	5.31	92.3	2.40	π*(dfppy)
	L	–1.92	2.04	6.34	91.6	π*(naftac)
	H	–5.44	50.8	42.9	6.32	d(Ir) + π(*dfppy*)
	H-1	–5.84	32.4	11.7	55.9	π(*natfac*) + d(Ir)
	H-2	–6.04	24.9	21.0	54.1	π(*natfac*) + d(Ir) + π(*dfppy*)
	H-3	–6.19	13.5	78.2	8.31	π(*dfppy*) + d(Ir)

[a] L = LUMO; H = HOMO.

Figure 7 shows the frontier orbital energy levels and energy gaps for the complexes. The HOMO of FIr(natfac) has the lowest energy (–5.44 eV) with relatively less d component and more contribution from dfppy. For the HOMO-1, the contributions are mainly from the metal d orbitals and π orbitals of ancillary ligands. FIr(natfac) has a lower HOMO-1 energy level than that of FIr(acac) and FIr(dbm), which may be due to electron-withdrawing effects and π-electron delocalization of the naphthyl group in FIr(natfac), as discussed above. However, the LUMOs of the complexes

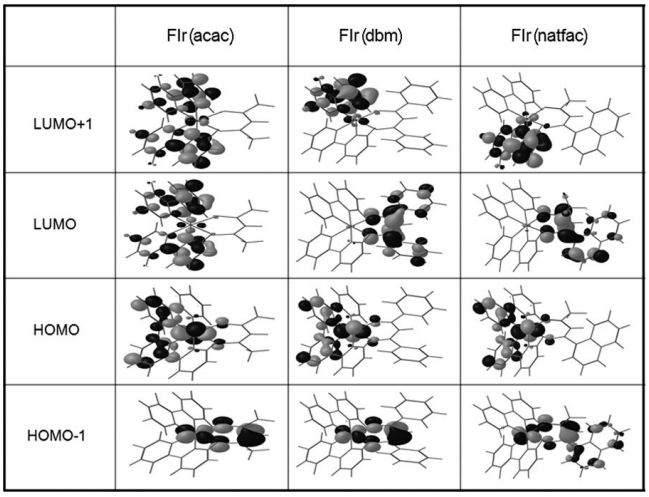

Figure 6. Contour plots of the frontier orbitals of complexes **1**–**3** in the ground state.

possess different π* character. The LUMO and LUMO+1 of FIr(acac) are degenerate orbitals which are mainly located on both the phenyl and pyridine moieties of the dfppy ligands, whereas the LUMOs of FIr(dbm) and FIr(natfac) are located on the ancillary ligands dbm and natfac, respectively, probably due to the lower LUMO energy of dbm and natfac. The LUMO energy levels of FIr(dbm) and FIr(natfac) decrease by 0.21 and 0.44 eV, respectively, with respect to that of FIr(acac). The trend in the calculated energy gaps is in good agreement with the values obtained electrochemically.

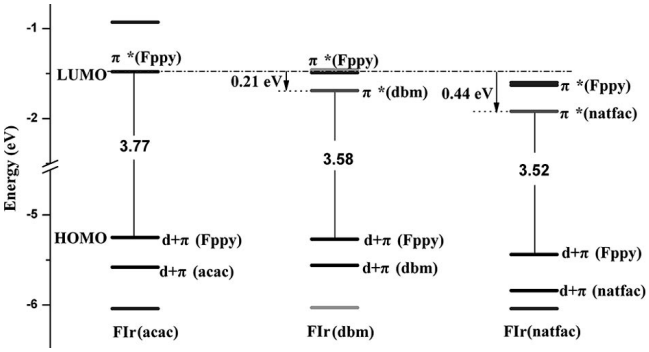

Figure 7. Frontier orbital energy levels and energy gaps of complexes **1**–**3**.

TD-DFT Calculations

TD-DFT calculations were employed to better understand the nature of the excited states and examine the vertical excitation energies for the allowed transitions between the low-lying excited states. The calculated excited energies, dominant orbital excitation, and oscillator strengths (*f*) for all three complexes are collected in Table 4; Figure 8 displays the main transitions contributing to the absorptions. The lowest transition-allowed singlet excited state with non-zero oscillator strength for FIr(acac), FIr(dbm), and FIr(natfac) is ascribed to the HOMO to LUMO+1 transition, with an absorption wavelength of 421, 419, and 413 nm,

Table 4. Calculated excited energies, dominant orbital excitation, and oscillator strength (*f*) from TD-DFT calculations for FIr(acac), FIr(dbm), and FIr(natfac).

State	Excitation	E_{cal} [eV]	λ_{cal} [nm]	*f*	λ_{exp}[a] [nm]	Character
FIr(acac)						
S_1	H → L+1(0.66)	2.94	421	0.0339	390	Ir/dfppy → dfppy(MLCT/ILCT)
S_3	H-1 → L(0.67)	3.32	373	0.0343		acac/Ir → dfppy(LLCT/MLCT)
S_6	H → L+2(0.66)	3.56	348	0.0181		Ir/dfppy → dfppy(MLCT/ILCT)
S_8	H-2 → L+1(0.61)	3.74	331	0.0686		dfppy → dfppy(ILCT)
S_9	H-2 → L(0.45)	3.78	328	0.0125		dfppy → dfppy(ILCT)
FIr(dbm)						
S_2	H → L+1(0.64)	2.83	419	0.0298	390	Ir/dfppy → dfppy(MLCT/ILCT)
S_4	H-1 → L(0.65)	3.22	385	0.0749		dbm/Ir → dbm(ILCT/MLCT)
S_5	H-1 → L+1(0.64)	3.32	373	0.0128		dbm/Ir → dfppy(LLCT/MLCT)
S_6	H-1 → L+2(0.63)	3.37	368	0.0105		dbm/Ir → dfppy(LLCT/MLCT)
S_7	H → L+3(0.69)	3.58	346	0.0147		Ir/dfppy → dfppy(MLCT/ILCT)
S_8	H-2 → L(0.61)	3.62	343	0.0992		dfppy/Ir → dbm(LLCT/MLCT)
S_{10}	H-2 → L+1(0.57)	3.72	333	0.0536		dfppy/Ir → dfppy(ILCT/MLCT)
FIr(natfac)						
S_2	H → L+1(0.61)	3.00	413	0.0297		Ir/dfppy → dfppy(MLCT/ILCT)
S_4	H-1 → L(0.62)	3.21	386	0.0665		natfac/Ir → natfac(ILCT/MLCT)
S_5	H-2 → L(0.57)	3.43	361	0.1956		natfac/Ir → natfac(ILCT/MLCT)
S_6	H-1 → L+1(0.57)	3.46	358	0.0309		natfac/Ir → dfppy(LLCT/MLCT)
S_7	H-1 → L+2(0.55)	3.53	351	0.0096		natfac/Ir → dfppy(LLCT/MLCT)
S_8	H-4 → L(0.42)	3.63	341	0.0127		dfppy/Ir → dfppy(ILCT/MLCT)
S_9	H → L+3(0.66)	3.64	340	0.0171		Ir/dfppy → dfppy(MLCT/ILCT)

[a] Experimental data of this work as can be seen from Figure 2.

respectively. The calculated absorption wavelengths are in good agreement with the experimental measurement (around 390 nm), with a deviation of about 30 nm. The reason for the difference between the experimental and calculated values is that our calculation is based on the gas-phase structure and ignores solvent effects. The transition characteristics for the absorption are ascribed to a mixed metal-to-ligand charge transfer (MLCT) and intra-ligand charge transfer (ILCT) state, as can be seen from the compositions of the HOMO and LUMO+1 orbitals for the three complexes. The transition occurs from the d orbitals of Ir and the π orbitals of dfppy to the π* orbitals of dfppy. The ancillary ligands are involved in the transitions at higher energy states, such as S_3 for FIr(acac).

For the emission properties, we should point out that the present calculations are based on the ground-state geometry assuming that there are no significant geometry changes between the excited state and ground state. The emission profiles are shown in Figure 9. The lowest triplet excited energies of the three complexes are 461, 505, and 513 nm respectively (see Table 5). In FIr(acac), the transition at 461 nm is attributed to a HOMO → LUMO+1 transition, which is consistent with the lowest singlet excitation, whereas the transitions for FIr(dbm) and FIr(natfac) are ascribed to HOMO-1 → LUMO transitions with a [d(Ir) + π(L^X) → π*(L^X)] character. We can therefore conclude that FIr(dbm) and FIr(natfac) have similar emission properties.

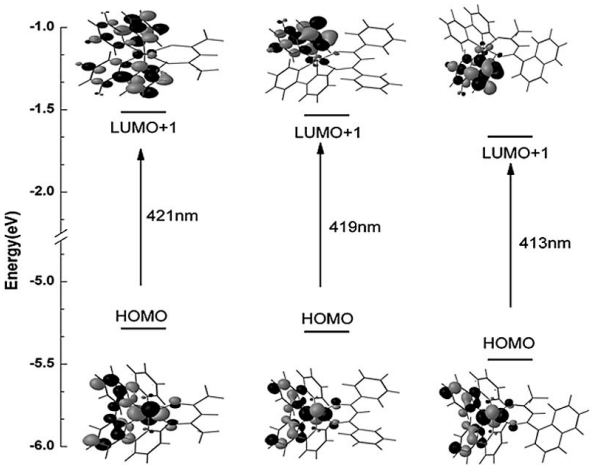

Figure 8. Transitions contributing to the absorptions at 421, 419, and 413 nm for FIr(acac), FIr(dbm), and FIr(natfac), respectively.

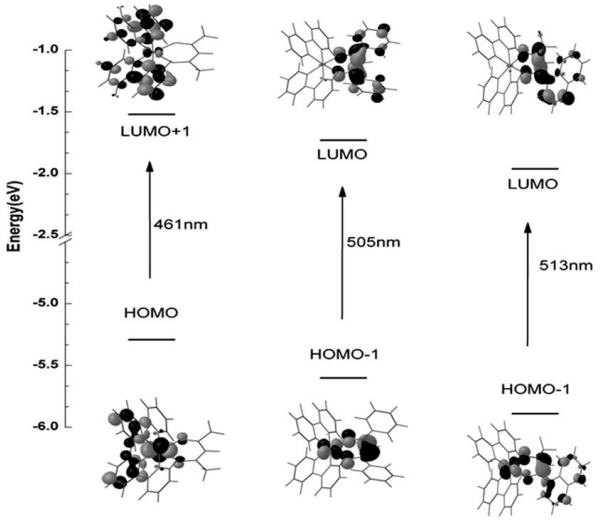

Figure 9. Transitions contributing to the emissions at 461, 505, and 513 nm for FIr(acac), FIr(dbm), and FIr(natfac), respectively.

Table 5. Calculated excited energies and dominant orbital excitation from TD-DFT calculations for complexes FIr(acac), FIr(dbm), and FIr(natfac).

State	Excitation	E_{cal} [eV]	λ_{cal} [nm]	λ_{exp}[a] [nm]	Character
FIr(acac)					
T_1	H → L+1(0.64)	2.69	461	482	Ir/dfppy → dfppy(MLCT/ILCT)
T_2	H → L(0.64)	2.70	459		Ir/dfppy → dfppy(MLCT/ILCT)
T_3	H-1 → L+3(0.66)	2.96	418		acac/Ir → acac(ILCT/MLCT)
FIr(dbm)					
T_1	H-1 → L(0.69)	2.45	505	557	dbm/Ir → dbm(ILCT/MLCT)
T_2	H → L+1(0.49)	2.71	457		Ir/dfppy → dfppy(MLCT/ILCT)
T_3	H → L(0.37)	2.76	450		Ir/dfppy → dfppy(MLCT/ILCT)
FIr(natfac)					
T_1	H-1 → L(0.65)	2.42	513	586	natfac/Ir → natfac(ILCT/MLCT)
T_2	H-2 → L(0.52)	2.59	478		natfac/Ir → natfac(ILCT/MLCT)
T_3	H → L(0.57)	2.69	462		dfppy/Ir → dfppy(ILCT/MLCT)

[a] Experimental data of this work as can be seen from Figure 3 and Table 1.

Experimentally, the efficiencies of FIr(dbm) and FIr(natfac) are so poor that they could not be measured. For FIr(acac), however, the phosphorescence efficiency in the film is 75%.[23] These results can be rationalized by considering that inefficient radiation transition might occur during the ILCT processes. All the ILCTs in dfppy occur during the absorption process. During the emission process, although ILCTs occur in dmb and natfac, these ligands experience structural relaxation and redistribution of electron densities and hence energy will dissipate during system crossing from singlet to triplet excited states through the vibrational motions, thus leading to radiationless transitions.

The calculated emission wavelengths are obviously hypsochromic with respect to the experimental measurements in films. There are two possible reasons for this. First of all, our calculations for the emission are based on the assumption that the geometry does not change much between ground and excited states. It is well accepted that excited-state structures are quite difficult to optimize for metal complexes. Previous calculations based on this hypothesis were adopted to simulate the emission properties.[18a,24] Furthermore, solvent effects should be taken into account.[25] For high accuracy, relativity effects, including spin-orbital coupling for the metal complexes, must be carefully considered.[26]

Conclusions

In summary, this work has demonstrated a simple method for tuning the emission color of metal complexes by changing the structures of the ancillary ligands. Furthermore, we have shown how the nature of substituents with electron-donating and electron-withdrawing groups can significantly influence the photophysical properties of [Ir(dfppy)$_2$(L^X)] complexes. By combining experimental results with DFT calculations, we have determined the detailed electronic structures and complicated absorption and emission process involved. For the emission, the transition of FIr(acac) is [d(Ir) + π (C^N) → π*(C^N)], whereas for FIr(dbm) and FIr(natfac) it is [d(Ir) + π (L^X) → π*(L^X)]. We have also shown that all of the low-lying excitations calculated in this study are MLCT and ILCT in nature. The properties of the complexes are affected by both the C^N and L^X ligands. Although the performance of these Ir^{III} complexes is far from good, it is possible that tuning the emission color can be achieved by systematically employing various distinctive ancillary ligands.

Experimental Section

General Procedures for Synthesis of Iridium Complexes: The cyclometalated chloride-bridged dimer [(dfppy)$_2$Ir(μ-Cl)$_2$Ir(dfppy)$_2$] was synthesized according to the procedure described in the literature by refluxing $IrCl_3 \cdot nH_2O$ with 2–2.5 equiv. of ligand in a 3:1 mixture of 2-ethoxyethanol and water. The chloride-bridged dimer complex (0.04 mmol), 0.12 mmol of acetyl acetone (dibenzoylmethanate, 1-naphthoyl-3,3,3-trifluoroacetone), and 0.36 mmol of sodium carbonate were then refluxed in 2-ethoxythanol for 15 h under nitrogen. After cooling to room temperature, the resulting precipitate was filtered off and washed with water and diethyl ether. The crude product was subjected to column chromatography on silica gel, eluting with dichloromethane, to provide the desired product in quantitative yield.

FIr(acac): ^{1}H NMR (500 MHz, [D$_6$]DMSO): δ = 8.43 (d, J = 5.6 Hz, 2 H), 8.23 (d, J = 8.4 Hz, 2 H), 8.07 (t, J = 8.0 Hz, 2 H), 7.50 (t, J = 7.1 Hz, 2 H), 6.69 (m, 2 H), 5.51 (dd, J = 8.7, 2.2 Hz, 2 H), 5.31 (s, 1 H), 1.76 (s, 6 H) ppm. IR (KBr): $\tilde{\nu}$ = 3068 (m), 1604 (s), 1574 (s), 1516 (m), 1479 (m), 1403 (s), 1291 (m), 1162 (m), 1102 (m) cm^{-1}. MALDI-TOF-MS: m/z 672.7 [M + H]$^+$. $C_{27}H_{19}F_4IrN_2O_2$ (671.67) calcd. C 48.28, H 2.85, N 4.17; found C 48.36, H 2.77, N 4.33.

FIr(dbm): ^{1}H NMR (500 MHz, [D$_6$]DMSO): δ = 8.49 (d, J = 5.6 Hz, 2 H), 8.26 (d, J = 8.4 Hz, 2 H), 8.05 (t, J = 7.7 Hz, 2 H), 7.81 (t, J = 7.6 Hz, 4 H), 7.49 (m, 4 H), 7.39 (t, J = 7.6 Hz, 4 H), 6.76 (t, J = 10.1 Hz, 2 H), 6.70 (s, 1 H), 6.65 (dd, J = 8.6, 1.9 Hz, 2 H) ppm. IR (KBr): $\tilde{\nu}$ = 3059 (m), 1064 (s), 1542 (s), 1521 (s), 1479 (s), 1404 (s), 1292 (m), 1163 (m), 1101 (m) cm^{-1}. MALDI-TOF-MS: m/z 796.8 [M + H]$^+$. $C_{37}H_{23}F_4IrN_2O_2$ (795.82) calcd. C 55.84, H 2.91, N 3.52; found C 55.98, H 2.93, N 3.50.

FIr(natfac): ^{1}H NMR (500 MHz, [D$_6$]DMSO): δ = 8.62 (s, 1 H), 8.44 (dd, J = 13.1, 5.0 Hz, 2 H), 8.29 (m, 2 H), 8.08 (m, 3 H), 7.92 (m, 2 H), 7.71 (dd, J = 8.6, 1.7 Hz, 1 H),7.65 (t, J = 7.6 Hz, 1 H), 7.58 (m, 2 H), 7.51 (t, J = 6.7 Hz, 1 H), 6.82 (m, 2 H), 6.66 (s, 1 H), 5.66 (dd, J = 8.6, 2.3 Hz, 1 H), 5.56 (dd, J = 8.6, 2.3 Hz, 1 H)

ppm. IR (KBr): $\tilde{\nu}$ = 3062 (m), 1604 (s), 1574 (s), 1479 (m), 1404 (m), 1296 (s), 1200 (m), 1162 (m), 1103 (m) cm^{-1}. MALDI-TOF-MS: *m*/*z* 838.7 $[M + H]^+$. $C_{36}H_{20}F_7IrN_2O_2$ (837.78): calcd. C 51.61, H 2.41, N 3.34; found C 51.74, H 2.59, N 3.45.

Physical Measurements: UV/Vis absorption spectra were recorded with a UV-3100 spectrophotometer. Photoluminescence measurements were performed with a RF-5301PC fluorometer. The electrochemical properties of these complexes were studied by cyclic voltammetry (CV) with ferrocene as the internal standard and an acetonitrile solution of the complexes containing 0.1 M tetrabutylammonium hexafluorophosphate as the supporting electrolyte at a scan rate of 100 $mV s^{-1}$. In all cases, potentials refer to the system Ag/0.1 M $AgNO_3$ in acetonitrile calibrated vs. the ferrocene redox couple. The HOMO and LUMO energy levels were determined using the following formula: $E_{HOMO} = -(E^{Ox}$ onset + 4.60) eV, $E_{LUMO} = -(E^{Red}$ onset + 4.60) eV.

Computational Details: DFT calculations were performed with the B3LYP[27] functional and the mixed "Double-ζ" quality basis sets 6-31G(d)[28] for the ligands and LANL2DZ for Ir. A relativistic effective core potential (ECP)[29] on Ir replaced the inner core electrons leaving the outer core $[(5s)^2(5p)^6]$ electrons and the $(5d^6)$ valence electrons of Ir^{III}. Optimization of the complexes was performed without any constraints for all three complexes. According to a previous study,[30] only the most stable structures, with the two N atoms from the dfppy ligands at *trans* positions, were considered. TD-DFT calculations were performed with the ground-state geometry to obtain the vertical excitation energies of the low-lying singlet and triplet excited states of the complexes. The B3LYP function with a larger 6-31+G(d) basis set was used for the ligands, with diffuse functions added to all lighter atoms except hydrogen.[24a,31] It is important to use basis sets with diffuse functions for systems in their excited states.[32] The lowest 10 triplet and 10 singlet states were obtained and compared with the absorption and phosphorescent spectra. All calculations were carried out using Gaussian 03.[33]

CCDC-727036 (for FIrdbm) contain the supplementary crystallographic data. These data can be obtained free of charge from the Cambridge Crystallographic Data Centre via www.ccdc.cam.ac.uk/data_request/cif.

Acknowledgments

We thank the National Nature Science Foundation of China (grant numbers 20573040, 20474024, 20603013, 20704015, 90501001, and 50303007), the Ministry of Science and Technology of China (grant number 2002CB6134003), and the Program for Changjiang Scholars and Innovative Research Team in University (PCSIRT) for financial support. Computational resources from in the Institute of Theoretical Chemistry at Jilin University are highly appreciated.

[1] a) E. Holder, B. M. W. Langeveld, U. S. Schubert, *Adv. Mater.* **2005**, *17*, 1109–1121; b) P.-T. Chou, Y. Chi, *Chem. Eur. J.* **2007**, *13*, 380–395.

[2] a) C. Adachi, M. A. Baldo, M. E. Thompson, S. R. Forrest, *J. Appl. Phys.* **2001**, *90*, 5048–5051; b) F. C. Chen, Y. Yang, *Appl. Phys. Lett.* **2002**, *80*, 2308–2310.

[3] a) M. G. Colombo, H. U. Güdel, *Inorg. Chem.* **1993**, *32*, 3081–3087; b) G. F. Strouse, H. U. Güdel, V. Bertolasi, V. Ferretti, *Inorg. Chem.* **1995**, *34*, 5578–5587; c) H. Wiedenhofer, S. Schützenmeier, A. V. Zelewsky, H. Yersin, *J. Phys. Chem.* **1995**, *99*, 13385–13391; d) J. Schmidt, H. Wiedenhofer, A. V. Zelewsky, H. Yersin, *J. Phys. Chem.* **1995**, *99*, 13385–13391.

[4] a) Y. Amao, Y. Ishikawa, I. Okura, *Anal. Chim. Acta* **2001**, *445*, 177–182; b) Y. Tang, E. C. Tehan, Z. Tao, F. V. Bright, *Anal. Chem.* **2003**, *75*, 2407–2413; c) M. C. DeRosa, P. J. Mosher, G. P. A. Yap, K.-S. Focsaeanu, R. J. Crutchley, C. E. B. Evans, *Inorg. Chem.* **2003**, *42*, 4864–4872; d) B. Lei, B. Li, H. Zhang, S. Lu, Z. Zheng, W. Li, Y. Wang, *Adv. Funct. Mater.* **2006**, *16*, 1883–1891.

[5] a) C. Adachi, M. A. Baldo, S. R. Forrest, S. Lamansky, M. E. Thompson, R. C. Kwong, *Appl. Phys. Lett.* **2001**, *78*, 1622–1624; b) S. Lamansky, P. Djurovich, D. Murphy, F. Abdel-Razzaq, H.-E. Lee, C. Adachi, P. E. Burrows, S. R. Forrest, M. E. Thompson, *J. Am. Chem. Soc.* **2001**, *123*, 4304–4312; c) S. Bettington, M. Tavasli, M. R. Bryce, A. Beeby, H. Al-Attar, A. P. Monkman, *Chem. Eur. J.* **2007**, *13*, 1423–1431; d) P. Wang, Y. Chuai, C. Chai, F. Wang, G. Zhang, G. Ge, X. Fan, H. Guo, D. Zou, Q. Zhou, *Polymer* **2008**, *49*, 455–460; e) J. O. Huh, M. H. Lee, H. Jang, K. Y. Hwang, J. S. Lee, S. H. Kim, Y. Do, *Inorg. Chem.* **2008**, *47*, 6566–6568.

[6] a) M. A. Baldo, M. E. Thompson, S. R. Forrest, *Nature* **2000**, *403*, 750–753; b) S. C. Lo, N. A. H. Male, J. P. J. Markham, S. W. Magennis, P. L. Burn, O. V. Salata, I. D. W. Samuel, *Adv. Mater.* **2002**, *14*, 975–979; c) A. B. Tamayo, B. D. Alleyne, P. I. Djurovich, S. Lamansky, I. Tsyba, N. N. Ho, R. Bau, M. E. Thompson, *J. Am. Chem. Soc.* **2003**, *125*, 7377–7387; d) S.-J. Yeh, M.-F. Wu, C.-T. Chen, Y.-H. Song, Y. Chi, M.-H. Ho, S.-F. Hsu, C. H. Chen, *Adv. Mater.* **2005**, *17*, 285–289; e) C.-H. Yang, Y. M. Cheng, Y. Chi, C.-J. Hsu, F.-C. Fang, K.-T. Wong, P.-T. Chou, C.-H. Chang, M.-H. Tsai, C.-C. Wu, *Angew. Chem. Int. Ed.* **2007**, *46*, 2418–2421; f) G. Zhou, Q. Wang, C.-L. Ho, W.-Y. Wong, D. Ma, L. Wang, Z. Lin, *Chem. Asian J.* **2008**, *3*, 1830–1841; g) V. L. Whittle, J. A. G. Williams, *Inorg. Chem.* **2008**, *47*, 6596–6607.

[7] a) B. Balzani, A. Juris, *Coord. Chem. Rev.* **2001**, *211*, 97–115; b) S. Welter, K. Brunner, J. W. Hofstraat, L. De Cola, *Nature* **2003**, *421*, 54–57.

[8] a) Y.-L. Tung, S.-W. Lee, Y. Chi, Y.-T. Tao, C.-H. Chien, Y.-M. Cheng, P.-T. Chou, S.-M. Peng, C.-S. Liu, *J. Mater. Chem.* **2005**, *15*, 460–464; b) F.-C. Hsu, Y.-L. Tung, Y. Chi, C.-C. Hsu, Y.-M. Cheng, M.-L. Ho, P.-T. Chou, S.-M. Peng, A. J. Carty, *Inorg. Chem.* **2006**, *45*, 10188–10196.

[9] a) M. K. Nazeeruddin, R. Humphry-Baker, D. Berner, S. Rivier, L. Zuppiroli, M. Graetzel, *J. Am. Chem. Soc.* **2003**, *125*, 8790–8797; b) C.-L. Li, Y.-J. Su, Y.-T. Tao, P.-T. Chou, C.-H. Chien, C.-C. Cheng, R.-S. Liu, *Adv. Funct. Mater.* **2005**, *15*, 387–395; c) D. K. Rayabarapu, B. M. J. S. Paulose, J.-P. Duan, C.-H. Cheng, *Adv. Mater.* **2005**, *17*, 349–353; d) H.-C. Li, P.-T. Chou, Y.-H. Hu, Y.-M. Liu, R.-S. Liu, *Organometallics* **2005**, *24*, 1329–1335; e) S. Okada, K. Okinaka, H. Iwawaki, M. Furugori, M. Hashimoto, T. Mukaide, J. Kamatani, S. Igawa, A. Tsuboyama, T. Takiguchi, K. Ueno, *Dalton Trans.* **2005**, *9*, 1583–1590; f) W.-Y. Wong, G.-J. Zhou, X.-M. Yu, H.-S. Kwok, B.-Z. Tang, *Adv. Funct. Mater.* **2006**, *16*, 838–846.

[10] a) A. Beeby, S. Bettington, I. D. W. Samuel, Z. J. Wang, *J. Mater. Chem.* **2003**, *13*, 80–83; b) S. Jung, Y. Kang, H.-S. Kim, Y.-H. Kim, C.-L. Lee, J.-J. Kim, S.-K. Lee, S.-K. Kwon, *Eur. J. Inorg. Chem.* **2004**, 3415–3423; c) B. Liang, C. Jiang, Z. Chen, X. Zhang, H. Shi, Y. Cao, *J. Mater. Chem.* **2006**, *16*, 1281–1286.

[11] a) C. Lee, R. R. Das, J. Kim, *Chem. Mater.* **2004**, *16*, 4642–4646; b) K. Dedeian, J. Shi, N. Shepherd, E. Forsythe, D. C. Morton, *Inorg. Chem.* **2005**, *44*, 4445–4447; c) F.-M. Hwang, H.-Y. Chen, P.-S. Chen, C.-S. Liu, Y. Chi, C.-F. Shu, F.-L. Wu, P.-T. Chou, S.-M. Peng, G.-H. Lee, *Inorg. Chem.* **2005**, *44*, 1344–1353; d) Y.-Y. Lyu, Y. Byun, O. Kwon, E. Han, W. S. Jeon, R. R. Das, K. Char, *J. Phys. Chem. B* **2006**, *110*, 10303–10314; e) S.-Y. Akizawa, J.-I. Nishida, T. Tsuzuki, S. Tokito, Y. Yamashita, *Inorg. Chem.* **2007**, *46*, 4308–4319; f) Y. Byun, W. S. Jeon, T.-W. Lee, Y.-Y. Lyu, S. Chang, O. Kwon, E. Han, H. Kim, M. Kim, H.-J. Lee, R. R. Das, *Dalton Trans.* **2008**, 4732–4741; g) D. D. Censo, S. Fantacci, F. D. Angelis, C. Klein, N.

Evans, K. Kalyanasundaram, H. J. Bolink, M. Gratzel, M. K. Nazeeruddin, *Inorg. Chem.* **2008**, *47*, 980–989.
[12] a) P. Coppo, E. A. Plummer, L. De Cola, *Chem. Commun.* **2004**, *15*, 1774–1775; b) A. Tsuboyama, H. Iwawaki, M. Furugori, T. Mukaide, J. Kamatani, S. Igawa, T. Moriyama, S. Miura, T. Takiguchi, S. Okada, M. Hoshino, K. Ueno, *J. Am. Chem. Soc.* **2003**, *125*, 12971–12979; c) T.-H. Kwon, H. S. Cho, M. K. Kim, J.-W. Kim, J.-J. Kim, K. H. Lee, S. J. Park, I.-S. Shin, H. Kim, D. M. Shin, Y. K. Chung, J.-I. Hong, *Organometallics* **2005**, *24*, 1578–1585; d) T. Sajoto, D. A. Tamayo, M. Yousufuddin, R. Bau, M. E. Thompaon, R. J. Holmes, S. R. Forrest, *Inorg. Chem.* **2005**, *44*, 7992–8003.
[13] Y. You, S. Y. Park, *J. Am. Chem. Soc.* **2005**, *127*, 12438–12439.
[14] C.-J. Chang, C.-H. Yang, K. Chen, Y. Chi, C.-F. Shu, M.-L. Ho, Y.-S. Yeh, P.-T. Chou, *Dalton Trans.* **2007**, 1881–1890.
[15] J. Li, P. I. Djurovich, B. D. Alleyne, M. Yousufuddin, N. N. Ho, J. C. Thomas, J. Peters, R. Bau, M. E. Thompson, *Inorg. Chem.* **2005**, *44*, 1713–1727.
[16] X. Gu, T. Fei, H. Y. Zhang, H. Xu, B. Yang, Y. G. Ma, X. D. Liu, *J. Phys. Chem. A* **2008**, *112*, 8387–8393.
[17] a) M. Polson, M. Ravaglia, S. Fracasso, M. Garavelli, F. Scandola, *Inorg. Chem.* **2005**, *44*, 1282–1289; b) A. B. Tamayo, S. Garon, T. Sajoto, P. I. Djurovich, I. M. Tsyba, R. Bau, M. E. Thompson, *Inorg. Chem.* **2005**, *44*, 8723–8732; c) S. C. Lo, C. P. Shipley, R. N. Bera, R. E. Harding, A. R. Cowley, P. L. Burn, I. D. W. Samuel, *Chem. Mater.* **2006**, *18*, 5119–5129; d) Q. Zhao, S. Liu, M. Shi, C. Wang, M. Yu, L. Li, F. Li, T. Yi, C. Huang, *Inorg. Chem.* **2006**, *45*, 6152–6160; e) I. Avilov, P. Minoofar, J. Cornil, L. D. Cola, *J. Am. Chem. Soc.* **2007**, *129*, 8247–8258.
[18] a) P. J. Hay, *J. Phys. Chem. A* **2002**, *106*, 1634–1641; b) C.-H. Yang, S.-W. Li, Y. Chi, Y.-M. Cheng, Y.-S. Yeh, P.-T. Chou, G.-H. Lee, C. H. Wang, C. F. Shu, *Inorg. Chem.* **2005**, *44*, 7770–7780; c) C. H. Yang, W. L. Su, K. H. Fang, S. P. Wang, I. W. Sun, *Organometallics* **2006**, *25*, 4514–4519; d) S. Obara, M. Itabashi, F. Okuda, S. Tamaki, Y. Tanabe, Y. Ishii, K. Nozaki, M.-A. Haga, *Inorg. Chem.* **2006**, *45*, 8907–8921; e) T. Liu, H.-X. Zhang, B.-H. Xia, *J. Phys. Chem. A* **2007**, *111*, 8724–8730.
[19] S. Lamansky, P. Djurovich, D. Murphy, F. Abdel-Razzaq, H.-E. Lee, C. Adachi, P. E. Burrows, S. R. Forrest, M. E. Thompson, *J. Am. Chem. Soc.* **2001**, *123*, 4304–4312.
[20] Standard deviations were calculated using the formula

$$\sigma = \sqrt{\frac{1}{N}\sum_{i=1}^{N}(x_i - x_{\exp})^2}$$

where x_i is the calculated result for each parameter, $x_{\exp}$ is the experimental value for the same parameter as x_i, and N is the total number of parameters selected for the calculations.
[21] N. G. Park, G. C. Choi, Y. H. Lee, Y. S. Kim, *Curr. Appl. Phys.* **2006**, *6*, 620–626.
[22] C. Dragonetti, L. Falciola, P. Mussini, S. Righetto, D. Roberto, R. Ugo, A. Valore, *Inorg. Chem.* **2007**, *46*, 8533–8547.
[23] FIr(acac) was dispersed in the inert host poly(methyl methacrylate) at 8.0 wt.-% and η_{PL} for the film was measured by an integrating sphere, using tris(8-quinolinolato)aluminum(III) as the standard fluorescent emitter. Tris(8-quinolinolato)aluminum(III) has a η_{PL} of 20(±1)% in our system.
[24] a) J.-F. Guillemoles, V. Barone, L. Joubert, C. Adamo, *J. Phys. Chem. A* **2002**, *106*, 11354–11360; b) X. Liu, J. Feng, A. Ren, L. Yang, B. Yang, Y. Ma, *Optical Mater.* **2006**, *29*, 231–238.
[25] a) M. K. Nazeeruddin, F. De Angelis, S. Fantacci, A. Selloni, G. Viscardi, P. Liska, S. Ito, B. Takeru, M. Grätzel, *J. Am. Chem. Soc.* **2005**, *127*, 16835–16847; b) Y. Xu, W.-K. Chen, M. J. Cao, S.-H. Liu, J.-Q. Li, A. I. Philippopoulos, P. Falaras, *Chem. Phys.* **2006**, *330*, 201–211; c) L.-C. Xu, S. Shi, J. Li, S.-Y. Liao, K.-C. Zheng, L.-N. Ji, *Dalton Trans.* **2008**, 291–301; d) T. Liu, X. Zhang, H.-X. Zhang, B.-H. Xia, *Dalton Trans.* **2008**, 1065–1072.
[26] a) T. Matsushita, T. Asada, S. Koseki, *J. Phys. Chem. C* **2007**, *111*, 6897–6903; b) E. Jansson, B. Minaev, S. Schrader, H. Agren, *Chem. Phys.* **2007**, *333*, 157–167.
[27] a) C. Lee, W. Yang, R. G. Parr, *Phys. Rev. B* **1998**, *37*, 785–789; b) A. D. Becke, *J. Chem. Phys.* **1993**, *98*, 5648–5653.
[28] A. E. Frisch, M. J. Frisch, *Gaussian 98 User's Reference*, Gaussian, Inc., Pittsburgh, PA, **1998**, and references cited therein.
[29] a) W. Koch, M. C. Holthausen, *A Chemist's Guide to Density Functional Theory*, Wiley-VCH, Weinheim, Germany, **2000**; b) C. Adamo, B. V. di Matteo, *Adv. Quantum Chem.* **1999**, *36*, 4–7.
[30] a) E. J. Nam, J. H. Kim, B. Kim, S. M. Kim, N. G. Park, Y. S. Kim, Y. K. Kim, Y. Ha, *Bull. Chem. Soc. Jpn.* **2004**, *77*, 751–755; b) Y. H. Lee, Y. S. Kim, *Curr. Appl. Phys.* **2007**, *7*, 504–508.
[31] a) H. H. Rho, G. Y. Park, Y. Ha, Y. S. Kim, *Jpn. J. Appl. Phys.* **2006**, *45*, 568–573; b) N. G. Park, G. C. Choi, J. E. Lee, Y. S. Kim, *Curr. Appl. Phys.* **2005**, *5*, 79–84.
[32] J. B. Foresman, A. E. Frisch, *Exploring Chemistry with Electronic Structure Methods*, 2nd ed., Gaussian, Inc., Pittsburgh, PA, **1996**, pp. 97–100.
[33] M. J. Frisch, G. W. Trucks, H. B. Schlegel, G. E. Scuseria, M. A. Robb, J. R. Cheeseman, J. A. Montgomery, T. Vreven Jr., K. N. Kudin, J. C. Burant, J. M. Millam, S. S. Iyengar, J. Tomasi, V. Barone, B. Mennucci, M. Cossi, G. Scalmani, N. Rega, G. A. Petersson, H. Nakatsuji, M. Hada, M. Ehara, K. Toyota, R. Fukuda, J. Hasegawa, M. Ishida, T. Nakajima, Y. Honda, O. Kitao, H. Nakai, M. Klene, X. Li, J. E. Knox, H. P. Hratchian, J. B. Cross, C. Adamo, J. Jaramillo, R. Gomperts, R. E. Stratmann, O. Yazyev, A. J. Austin, R. Cammi, C. Pomelli, J. W. Ochterski, P. Y. Ayala, K. Morokuma, G. A. Voth, P. Salvador, J. J. Dannenberg, V. G. Zakrzewski, S. Dapprich, A. D. Daniels, M. C. Strain, O. Farkas, D. K. Malick, A. D. Rabuck, K. Raghavachari, J. B. Foresman, J. V. Ortiz, Q. Cui, A. G. Baboul, S. Clifford, J. Cioslowski, B. B. Stefanov, G. Liu, A. Liashenko, P. Piskorz, I. Komaromi, R. L. Martin, D. J. Fox, T. Keith, M. A. Al-Laham, C. Y. Peng, A. Nanayakkara, M. Challacombe, P. M. W. Gill, B. Johnson, W. Chen, M. W. Wong, C. Gonzalez, J. A. Pople, *Gaussian 03 (Revision B05)*, Gaussian, Inc., Pittsburgh, PA, **2003**.

Received: December 7, 2008
Published Online: April 28, 2009

